PERGAMON

International Journal of Solids and Structures 40 (2003) 747–762

INTERNATIONAL JOURNAL OF SOLIDS and STRUCTURES

www.elsevier.com/locate/ijsolstr

Investigation of the dynamic behavior of two parallel symmetric cracks in piezoelectric materials use of non-local theory

Zhen-Gong Zhou *, Biao Wang, Yu-Guo Sun

Center for Composite Materials and Electro-Optics Research Center, Harbin Institute of Technology, P.O. Box 1247, Harbin 150001, PR China

Received 30 August 2001; received in revised form 26 August 2002

Abstract

In this paper, the dynamic behavior of two parallel symmetric cracks in piezoelectric materials under harmonic anti-plane shear waves is investigated by use of the non-local theory for permeable crack surface conditions. To overcome the mathematical difficulties, a one-dimensional non-local kernel is used instead of a two-dimensional one for the problem to obtain the stress occurs near the crack tips. By means of the Fourier transform, the problem can be solved with the help of two pairs of dual integral equations that the unknown variables are the jumps of the displacement along the crack surfaces. These equations are solved using the Schmidt method. Numerical examples are provided. Contrary to the previous results, it is found that no stress and electric displacement singularity is present near the crack tip. The non-local elastic solutions yield a finite hoop stress near the crack tip, thus allowing for a fracture criterion based on the maximum stress hypothesis. The finite hoop stress at the crack tip depends on the crack length, the frequency of the incident wave, the distance between two cracks and the lattice parameter of the materials, respectively. Contrary to the impermeable crack surface condition solution, it is found that the dynamic electric displacement for the permeable crack surface conditions is much smaller than the results for the impermeable crack surface conditions. The results show that the dynamic field will impede or enhance crack propagation in the piezoelectric materials at different stages of the dynamic load.

Keywords: Dynamic; Symmetric; Piezoelectric

1. Introduction

Piezoelectric materials produce an electric field when deformed, and undergo deformation when subjected to an electric field. The coupling nature of piezoelectric materials has attracted wide applications in electric-mechanical and electric devices, such as electric-mechanical actuators, sensors and structures. When

* Corresponding author. Tel.: +86-451-641-4145; fax: +86-451-623-8476.
E-mail address: zhouzhg@hope.hit.edu.cn (Z.-G. Zhou).

0020-7683/02/$ - see front matter © 2002 Elsevier Science Ltd. All rights reserved.
PII: S0020-7683(02)00592-9

subjected to mechanical and electrical loads in service, these piezoelectric materials can fail prematurely due to their brittleness and presence of defects or flaws produced during their manufacturing process. Therefore, it is important to study the electro-elastic interaction and fracture behaviors of piezoelectric materials. Moreover, it is known that the failure of solids results from the final propagation of the cracks, and in most cases, the unstable growth of the crack is brought about by the external dynamic loads. So, the study of the dynamic fracture mechanics of piezoelectric materials is much more importance in recent research, especially when multiple cracks are involved. From the viewpoint of fracture dynamics, the response of cracks under dynamic loads is more complex, particularly for piezoelectricity. In such a case, elastic wave is generated throughout the structure. Near the cracks, these waves are reflected and refracted causing the local stress to increase beyond its corresponding static value. This could lead to the unstable motion of the crack and eventually the fracture of the structure.

In the theoretical studies of crack problems, several different electric boundary conditions at the crack surfaces have been proposed by numerous researchers. For example, for the sake of analytical simplification, the assumption that the crack surfaces are impermeable to electric fields was adopted by Deeg (1980), Pak (1990, 1992), Sosa and Pak (1990), Sosa (1991, 1992), Suo et al. (1992), Gao et al. (1997). In this model, the assumption of the impermeable cracks refers to the fact that the crack surfaces are free of surface charge and thus the electric displacement vanishes insides the crack. In fact, cracks in piezoelectric materials consist of vacuum, air or some other gas. This requires that the electric fields can propagate through the crack, so the electric displacement component perpendicular to the crack surfaces should be continuous across the crack surfaces. Along this line, Zhang and Hack (1992) analyzed crack problems in piezoelectric materials. In addition, usually the conducting cracks which are filled with conducting gas or liquid are also applied to be a kind of simplified cracks models in piezoelectric materials by many researchers, such as McMeeking (1989) and Suo (1993). Recently, Dunn (1994), Zhang and Tong (1996), and Sosa and Khutoryansky (1999) avoided the common assumption of electric impermeability and utilized more accurate electric boundary conditions at the rim of an elliptical flaw to deal with anti-plane problems in piezoelectricity. They analyzed the effects of electric boundary conditions at the crack surfaces on the fracture mechanics of piezoelectric materials. It is interesting to note that very different results were obtained by changing the boundary conditions. Most recently, Soh et al. (2000) have investigated the behavior of a bi-piezoelectric ceramic layer with an interfacial crack by using the dislocation density function and the singular integral equation method for two different crack surface boundary conditions, respectively, i.e. permeable and impermeable. However, these solutions contain stress singularity. This is not reasonable according to the physical nature. To overcome the stress singularity in the classical elastic theory, Eringen (Eringen et al., 1977, Eringen, 1978, 1979) used non-local theory to discuss the state of stress near the tip of a sharp line crack in an elastic plate subject to uniform tension, shear and anti-plane shear. These solutions did not contain any stress singularity, thus resolving a fundamental problem that has remained unsolved for over many years. This enables us to employ the maximum stress hypothesis to deal with fracture problems in a natural way. Eringen (Eringen, 1984) has presented the general theory of non-local piezoelectricity. Recently, the same problems have been resolved in Zhou's papers (Zhou et al., 1998a, 1999b) by using the Schmidt method. In papers (Zhou et al., 1999a; Zhou et al., 1998b; Zhou et al., 1999c; Zhou and Shen, 1999; Zhou and Jia, 2000; Zhou et al., 2001), the problems for a crack or two cracks were investigated in the elastic materials or in the piezoelectric materials by use of non-local theory. To our knowledge, the dynamic electro-elastic behavior of the piezoelectric materials with two parallel cracks subjected to harmonic anti-plane shear waves has not been studied by use of non-local theory for permeable crack surface boundary conditions.

In the present paper, the dynamic behavior of two parallel symmetric cracks subjected to harmonic anti-plane shear waves in piezoelectric materials is investigated by means of non-local theory for permeable crack face conditions. The traditional concept of linear elastic fracture mechanics and non-local theory are extended to include the piezoelectric effects. To overcome the mathematical difficulties, one has to accept some assumptions as in Nowinski's works (Nowinski 1984a,b), a one-dimensional non-local kernel function is used instead of a two-dimensional kernel function for the anti-plane problem to obtain the stress near at the crack tips. Certainly, the assumption should be further investigated to satisfy the realistic condition. Fourier transform is applied and a mixed boundary value problem is reduced to two pairs of dual integral equations that the unknown variables are the jumps of the displacement along the crack surfaces. In solving the dual integral equations, the jumps of the crack surface displacement are expanded in a series of Jacobi polynomials. The Schmidt method (Morse and Feshbach, 1958) is used to obtain the solution. This process is quite different from that adopted in previous works (Han and Wang, 1999; Deeg, 1980; Pak, 1992; Sosa, 1992; Suo et al., 1992; Park and Sun, 1995; Zhang and Tong, 1996; Gao et al., 1997; Wang, 1992; Narita and Shindo, 1998; Chen et al., 1999; Shen et al., 1999; Shen et al., 2000; Kim and Jones, 1996; Beom and Atluri, 1996; Qin and Yu, 1997; Soh et al., 2000; Eringen et al., 1977; Eringen, 1978, 1979; Yu and Chen, 1998). As expected, the solution in this paper does not contain the stress and electric displacement singularity at the crack tip, thus clearly indicating the physical nature of the problem.

2. Basic equations of non-local piezoelectric materials

For the anti-plane shear problem, the basic equations of linear, homogeneous, isotropic, non-local piezoelectric materials, with vanishing body force are (see e.g. Eringen, 1979; Shindo et al., 1996)

$$\frac{\partial \tau_{xz}}{\partial x} + \frac{\partial \tau_{yz}}{\partial y} = \rho \frac{\partial^2 w}{\partial t^2}, \tag{1}$$

$$\frac{\partial D_x}{\partial x} + \frac{\partial D_y}{\partial y} = 0, \tag{2}$$

$$\tau_{kz}(X,t) = \int_V [c'_{44}(|X'-X|)w_{,k}(X',t) + e'_{15}(|X'-X|)\phi_{,k}(X',t)]\,\mathrm{d}V(X') \quad (k = x, y), \tag{3}$$

$$D_k(X,t) = \int_V [e'_{15}(|X'-X|)w_{,k}(X',t) - \varepsilon'_{11}(|X'-X|)\phi_{,k}(X',t)]\,\mathrm{d}V(X') \quad (k = x, y), \tag{4}$$

where the only difference with classical elastic theory and the piezoelectric theory is in the stress and the electric displacement constitutive equations (3) and (4) in which the stress $\tau_{zk}(X,t)$ and the electric displacement $D_k(X,t)$ at a point X depends on $w_{,k}(X,t)$ and $\phi_{,k}(X,t)$, at all points of the body. w and ϕ are the mechanical displacement and electric potential. ρ is the density of the piezoelectric materials. For homogeneous and isotropic piezoelectric materials there exist only three material parameters, $c'_{44}(|X'-X|)$, $e'_{15}(|X'-X|)$ and $\varepsilon'_{11}(|X'-X|)$ which are functions of the distance $|X'-X|$. The integrals in (3) and (4) are over the volume V of the body enclosed within a surface ∂V. As discussed in the papers (see e.g. Eringen, 1974, 1977), it can be assumed in the form of $c'_{44}(|X'-X|)$, $e'_{15}(|X'-X|)$ and $\varepsilon'_{11}(|X'-X|)$ for which the dispersion curves of plane elastic waves coincide with those known in lattice dynamics. Among several possible curves the following has been found to be very useful

$$(c'_{44}, e'_{15}, \varepsilon'_{11}) = (c_{44}, e_{15}, \varepsilon_{11})\alpha(|X'-X|), \tag{5}$$

$\alpha(|X'-X|)$ is known as the influence function, and is the functions of the distance $|X'-X|$. c_{44}, e_{15} and ε_{11} are shear modulus, piezoelectric coefficient and dielectric parameter, respectively. Substitution of Eq. (5) into Eqs. (3) and (4) yields

$$\tau_{kz}(X,t) = \int_V \alpha(|X' - X|)\sigma_{kz}(X',t)\,\mathrm{d}V(X') \quad (k = x, y), \tag{6}$$

$$D_k(X,t) = \int_V \alpha(|X' - X|)D_k^c(X',t)\,\mathrm{d}V(X') \quad (k = x, y), \tag{7}$$

where

$$\sigma_{kz} = c_{44}w_{,k} + e_{15}\phi_{,k} \quad (k = x, y), \tag{8}$$

$$D_k^c = e_{15}w_{,k} - \varepsilon_{11}\phi_{,k} \quad (k = x, y). \tag{9}$$

The expressions (8) and (9) are the classical constitutive equations.

3. The crack model

It is assumed that there are two parallel symmetric cracks of length $2l$ in the piezoelectric materials as shown in Fig. 1. h is the distance between the two cracks. The piezoelectric boundary-value problem for anti-plane shear is considerably simplified if we consider only the out-of-plane displacement and the in-plane electric fields. In this paper, the harmonic anti-plane shear wave is vertically incident. Let ω be the circular frequency of the incident wave. $-\tau_0$ is a magnitude of the incident wave. In what follows, the time-dependence of all field quantities assumed to be of the form $e^{-i\omega t}$ will be suppressed as commonly used technique. As discussed in Soh's (Soh et al., 2000), Srivastava's (Srivastava et al., 1983) and Eringen's (Eringen, 1979) works, since no opening displacement exists for the present anti-plane problem, the crack surfaces can be assumed to be in perfect contact. Accordingly, permeable condition will be enforced in the present study, i.e. both the electric potential and the normal electric displacement are assumed to be continuous across the crack surfaces. So the boundary conditions of the present problem are (in this paper, we only consider the perturbation stress field and the perturbation electric displacement field):

$$w^{(1)} = w^{(2)}, \quad \tau_{yz}^{(1)} = \tau_{yz}^{(2)}, \quad \phi^{(1)} = \phi^{(2)}, \quad D_y^{(1)} = D_y^{(2)}, \quad y = h, \ |x| > l, \tag{10}$$

$$w^{(2)} = w^{(3)}, \quad \tau_{yz}^{(2)} = \tau_{yz}^{(3)}, \quad \phi^{(2)} = \phi^{(3)}, \quad D_y^{(2)} = D_y^{(3)}, \quad y = 0, \ |x| > l, \tag{11}$$

$$\tau_{yz}^{(1)} = \tau_{yz}^{(2)} = -\tau_0, \quad \phi^{(1)} = \phi^{(2)}, \quad D_y^{(1)} = D_y^{(2)}, \quad y = h, \ |x| \leqslant l, \tag{12}$$

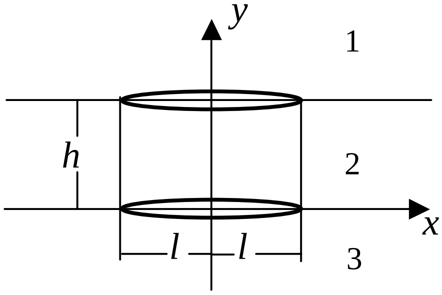

Fig. 1. Two parallel symmetric cracks in a piezoelectric material.

$$\tau_{yz}^{(2)} = \tau_{yz}^{(3)} = -\tau_0, \quad \phi^{(2)} = \phi^{(3)}, \quad D_y^{(2)} = D_y^{(3)}, \quad y = 0, \ |x| \leqslant l, \tag{13}$$

$$w^{(1)} = w^{(3)} = 0 \quad \text{for } (x^2 + y^2)^{1/2} \to \infty; \quad w^{(2)} = 0, \quad \text{for } |x| \to \infty, \tag{14}$$

where τ_{zk}, D_k $(k = x, y)$ are the anti-plane shear stress and in-plane electric displacement, respectively. w and ϕ are the mechanical displacement and the electric potential. Note that all quantities with superscript k $(k = 1, 2, 3)$ refer to the upper half plane 1, the layer 2 and the lower half plane 3 as in Fig. 1, respectively. In this paper, we only consider positive τ_0. Substituting Eqs. (6)–(9) into Eqs. (1) and (2), respectively, using Green–Gauss theorem leads to (see e.g. Eringen, 1979):

$$\int_V \int \alpha(|x'-x|, |y'-y|)[c_{44}\nabla^2 w(x', y', t) + e_{15}\nabla^2\phi(x', y', t)]\,\mathrm{d}x'\,\mathrm{d}y' - \int_{-l}^{l} \alpha(|x'-x|, 0)[\![\sigma_{yz}(x', 0, t)]\!]\,\mathrm{d}x' - \int_{-l}^{l} \alpha(|x'-x|, h)[\![\sigma_{yz}(x', h, t)]\!]\,\mathrm{d}x' = \rho\frac{\partial^2 w}{\partial t^2}, \tag{15}$$

$$\int_V \int \alpha(|x'-x|, |y'-y|)[e_{15}\nabla^2 w(x', y', t) - \varepsilon_{11}\nabla^2\phi(x', y', t)]\,\mathrm{d}x'\,\mathrm{d}y' - \int_{-l}^{l} \alpha(|x'-x|, 0)[\![D_y^c(x', 0, t)]\!]\,\mathrm{d}x' - \int_{-l}^{l} \alpha(|x'-x|, h)[\![D_y^c(x', h, t)]\!]\,\mathrm{d}x' = 0, \tag{16}$$

where the boldface bracket indicates a jump at the crack line, i.e.

$$\begin{aligned}
&[\![\sigma_{yz}(x', 0, t)]\!] = \sigma_{yz}(x', 0^+, t) - \sigma_{yz}(x', 0^-, t),\\
&[\![\sigma_{yz}(x', h, t)]\!] = \sigma_{yz}(x', h^+, t) - \sigma_{yz}(x', h^-, t),\\
&[\![D_y^c(x', 0, t)]\!] = D_y^c(x', 0^+, t) - D_y^c(x', 0^-, t),\\
&[\![D_y^c(x', h, t)]\!] = D_y^c(x', h^+, t) - D_y^c(x', h^-, t).
\end{aligned}$$

$\nabla^2 = \partial^2/\partial x^2 + \partial^2/\partial y^2$ is the two-dimensional Laplace operator. From the continuous conditions of the stress and the electric displacement, it can be obtained

$$[\![\sigma_{yz}(x, y, t)]\!] = 0, \quad [\![D_y^c(x, y, t)]\!] = 0. \tag{17}$$

Hence the line integrals in (15) and (16) vanish. By taking the Fourier cosine transform of (15) and (16) with respect to x', it can be shown that the general solutions of (15) and (16) are identical to that of

$$\int_0^\infty \bar{\alpha}(|s|, |y'-y|)\left\{c_{44}\left[\frac{\mathrm{d}^2\bar{w}(s, y', t)}{\mathrm{d}y^2} - s^2\bar{w}(s, y', t)\right] + e_{15}\left[\frac{\mathrm{d}^2\bar{\phi}(s, y', t)}{\mathrm{d}y^2} - s^2\bar{\phi}(s, y', t)\right]\right\}\mathrm{d}y' = \rho\omega^2\bar{w}, \tag{18}$$

$$\int_0^\infty \bar{\alpha}(|s|, |y'-y|)\left\{e_{15}\left[\frac{\mathrm{d}^2\bar{w}(s, y', t)}{\mathrm{d}y^2} - s^2\bar{w}(s, y', t)\right] - \varepsilon_{11}\left[\frac{\mathrm{d}^2\bar{\phi}(s, y', t)}{\mathrm{d}y^2} - s^2\bar{\phi}(s, y', t)\right]\right\}\mathrm{d}y' = 0. \tag{19}$$

Here a superposed bar indicates the Fourier cosine transform, i.e.

$$\bar{f}(s) = \int_0^\infty f(x)\cos(sx)\,\mathrm{d}x, \quad f(x) = \frac{2}{\pi}\int_0^\infty \bar{f}(s)\cos(sx)\,\mathrm{d}s.$$

What now remains is to solve the integrodifferential equations (18) and (19) for the function w and ϕ. It is impossible to obtain a rigorous solution at the present stage for Eqs. (18) and (19). It seems obvious that in the solution of such a problem we encounter serious if not unsurmountable mathematical difficulties and will have to resort to an approximate procedure. In the given problem, according to the assumptions as in Nowinski's works (Nowinski 1984a,b), the non-local interaction in y-direction can be ignored. It can be given

$$\bar{\alpha}(|s|, |y' - y|) = \bar{\alpha}_0(s)\delta(y' - y). \tag{20}$$

From Eqs. (18) and (19), we have

$$\bar{\alpha}_0(s)\left\{c_{44}\left[\frac{d^2\bar{w}(s,y,t)}{dy^2} - s^2\bar{w}(s,y,t)\right] + e_{15}\left[\frac{d^2\bar{\phi}(s,y,t)}{dy^2} - s^2\bar{\phi}(s,y,t)\right]\right\} = \rho\omega^2\bar{w}, \tag{21}$$

$$e_{15}\left[\frac{d^2\bar{w}(s,y,t)}{dy^2} - s^2\bar{w}(s,y,t)\right] - \varepsilon_{11}\left[\frac{d^2\bar{\phi}(s,y,t)}{dy^2} - s^2\bar{\phi}(s,y,t)\right] = 0. \tag{22}$$

The general solutions of the Eqs. (21) and (22) satisfying (14) are, respectively:

$$\begin{cases} w^{(1)}(x,y,t) = \dfrac{2}{\pi}\displaystyle\int_0^\infty A_1(s)e^{-\gamma y}\cos(sx)\,ds, \\ \phi^{(1)}(x,y,t) = \dfrac{e_{15}}{\varepsilon_{11}}w^{(1)}(x,y,t) + \dfrac{2}{\pi}\displaystyle\int_0^\infty B_1(s)e^{-sy}\cos(sx)\,ds, \end{cases} \quad (y \geqslant h) \tag{23}$$

$$\begin{cases} w^{(2)}(x,y,t) = \dfrac{2}{\pi}\displaystyle\int_0^\infty [A_2(s)e^{-\gamma y} + B_2(s)e^{\gamma y}]\cos(sx)\,ds, \\ \phi^{(2)}(x,y,t) = \dfrac{e_{15}}{\varepsilon_{11}}w^{(2)}(x,y,t) + \dfrac{2}{\pi}\displaystyle\int_0^\infty [C_2(s)e^{-sy} + D_2(s)e^{sy}]\cos(sx)\,ds, \end{cases} \quad (h \geqslant y \geqslant 0) \tag{24}$$

$$\begin{cases} w^{(3)}(x,y,t) = \dfrac{2}{\pi}\displaystyle\int_0^\infty A_3(s)e^{\gamma y}\cos(sx)\,ds, \\ \phi^{(3)}(x,y,t) = \dfrac{e_{15}}{\varepsilon_{11}}w^{(3)}(x,y,t) + \dfrac{2}{\pi}\displaystyle\int_0^\infty B_3(s)e^{sy}\cos(sx)\,ds, \end{cases} \quad (y \leqslant 0) \tag{25}$$

where $\gamma^2 = s^2 - \omega^2/c^2\bar{\alpha}_0(s)$, $\mu = c_{44} + (e_{15}^2/\varepsilon_{11})$, $c^2 = \mu/\rho$ is the stress wave velocity in the piezoelectric materials. $A_1(s)$, $B_1(s)$, $A_2(s)$, $B_2(s)$, $C_2(s)$, $D_2(s)$, $A_3(s)$ and $B_3(s)$ are to be determined from the boundary conditions. So from Eqs. (6)–(9), we have

$$\begin{cases} \tau_{yz}^{(1)} = -\dfrac{2}{\pi}\displaystyle\int_0^\infty \bar{\alpha}_0(s)[\mu\gamma A_1(s)e^{-\gamma y} + e_{15}sB_1(s)e^{-sy}]\cos(sx)\,ds, \\ D_y^{(1)} = \dfrac{2}{\pi}\displaystyle\int_0^\infty \bar{\alpha}_0(s)\varepsilon_{11}sB_1(s)e^{-sy}\cos(sx)\,ds, \end{cases} \quad (y \geqslant h) \tag{26}$$

$$\begin{cases} \tau_{yz}^{(2)} = -\dfrac{2}{\pi}\displaystyle\int_0^\infty \bar{\alpha}_0(s)\{\mu\gamma[A_2(s)e^{-\gamma y} - B_2(s)e^{\gamma y}] + e_{15}s[C_2(s)e^{-sy} - D_2(s)e^{sy}]\}\cos(sx)\,ds, \\ D_y^{(2)} = \dfrac{2}{\pi}\displaystyle\int_0^\infty \bar{\alpha}_0(s)\varepsilon_{11}s[C_2(s)e^{-sy} - D_2(s)e^{sy}]\cos(sx)\,ds, \end{cases} \quad (h \geqslant y \geqslant 0) \tag{27}$$

$$\begin{cases} \tau_{yz}^{(3)} = \dfrac{2}{\pi}\displaystyle\int_0^\infty \bar{\alpha}_0(s)[\mu\gamma A_3(s)e^{\gamma y} + e_{15}sB_3(s)e^{sy}]\cos(sx)\,ds, \\ D_y^{(3)} = -\dfrac{2}{\pi}\displaystyle\int_0^\infty \bar{\alpha}_0(s)\varepsilon_{11}sB_3(s)e^{sy}\cos(sx)\,ds. \end{cases} \quad (y \leqslant 0) \tag{28}$$

To solve the problem, the jump functions of the crack surface displacements and the electric potentials are defined as follows:

$$f_1(x) = w^{(1)}(x, h^+, t) - w^{(2)}(x, h^-, t), \tag{29}$$

$$f_{\phi 1}(x) = \phi^{(1)}(x, h^+, t) - \phi^{(2)}(x, h^-, t), \tag{30}$$

$$f_2(x) = w^{(2)}(x, 0^+, t) - w^{(3)}(x, 0^-, t), \tag{31}$$

$$f_{\phi 2}(x) = \phi^{(2)}(x, 0^+, t) - \phi^{(3)}(x, 0^-, t). \tag{32}$$

Substituting Eqs. (23)–(25) into Eqs. (29)–(32), and applying the Fourier transform and the boundary conditions, we have

$$\bar{f}_1(s) = [A_1(s) - A_2(s)]e^{-\gamma h} - B_2(s)e^{\gamma h}, \tag{33}$$

$$\bar{f}_{\phi 1}(s) = \frac{e_{15}}{\varepsilon_{11}}\bar{f}_1(s) + [B_1(s) - C_2(s)]e^{-sh} - D_2(s)e^{sh} = 0, \tag{34}$$

$$\bar{f}_2(s) = A_2(s) + B_2(s) - A_3(s), \tag{35}$$

$$\bar{f}_{\phi 2}(s) = \frac{e_{15}}{\varepsilon_{11}}\bar{f}_2(s) + C_2(s) + D_2(s) - B_3(s) = 0. \tag{36}$$

Substituting Eqs. (26)–(28) into Eqs. (10)–(13), it can be obtained

$$\mu\gamma A_1(s)e^{-\gamma h} + e_{15}sB_1(s)e^{-sh} = \mu\gamma[A_2(s)e^{-\gamma h} - B_2(s)e^{\gamma h}] + e_{15}s[C_2(s)e^{-sh} - D_2(s)e^{sh}], \tag{37}$$

$$[B_1(s) - C_2(s)]e^{-2sh} + D_2(s) = 0, \tag{38}$$

$$\mu\gamma[A_2(s) - B_2(s)] + e_{15}s[C_2(s) - D_2(s)] = -\mu\gamma A_3(s) - e_{15}sB_3(s), \tag{39}$$

$$C_2(s) - D_2(s) + B_3(s) = 0. \tag{40}$$

By solving eight equations (33)–(40) with eight unknown functions $A_1(s)$, $B_1(s)$, $A_2(s)$, $B_2(s)$, $C_2(s)$, $D_2(s)$, $A_3(s)$, $B_3(s)$ and applying the boundary conditions (10)–(13), it can be obtained:

$$\int_0^\infty \bar{\alpha}_0(s)\left\{\mu\gamma[\bar{f}_1(s) + e^{-\gamma h}\bar{f}_2(s)] - \frac{e_{15}^2}{\varepsilon_{11}}s[\bar{f}_1(s) + \bar{f}_2(s)e^{-sh}]\right\}\cos(sx)\,ds = \pi\tau_0, \quad |x| \leqslant l, \tag{41}$$

$$\int_0^\infty \bar{\alpha}_0(s)\left\{\mu\gamma[\bar{f}_2(s) + e^{-\gamma h}\bar{f}_1(s)] - \frac{e_{15}^2}{\varepsilon_{11}}s[\bar{f}_2(s) + \bar{f}_1(s)e^{-sh}]\right\}\cos(sx)\,ds = \pi\tau_0, \quad |x| \leqslant l, \tag{42}$$

$$\int_0^\infty \bar{f}_1(s)\cos(sx)\,ds = 0, \quad |x| > l, \tag{43}$$

$$\int_0^\infty \bar{f}_2(s)\cos(sx)\,ds = 0, \quad |x| > l. \tag{44}$$

From Eqs. (41)–(44), it can be found

$$\bar{f}_1(s) = \bar{f}_2(s) \Rightarrow f_1(x) = f_2(x), \quad \tau_{yz}^{(1)}(x, h, t) = \tau_{yz}^{(2)}(x, h, t) = \tau_{yz}^{(2)}(x, 0, t) = \tau_{yz}^{(3)}(x, 0, t) = \tau_{yz}. \tag{45}$$

So from Eqs. (26)–(28), it can be obtained $D_y^{(1)}(x, h, t) = D_y^{(2)}(x, h, t) = D_y^{(2)}(x, 0, t) = D_y^{(3)}(x, 0, t) = D_y$. To determine the unknown functions $\bar{f}_1(s)$ and $\bar{f}_2(s)$, the dual integral equations (41)–(44) must be solved.

4. Solution of the dual integral equations

Here, the only difference between the classical and non-local equations is in the introduction of the function $\bar{\alpha}_0(s)$, it is logical to utilize the classical solution to convert the system equations (41)–(44) to an integral equation of the second kind which is generally better behaved. If $\bar{\alpha}_0(s) = 1$ (the classical elastic case), Eqs. (41)–(44) reduce to the dual integral equations for the same problem in classical elasticity. The dual integral equations (41)–(44) cannot be transformed into a Fredholm integral equation of the second kind (Eringen, 1979), because the kernel of the Fredholm integral equation of the second kind in the paper of Eringen (Eringen, 1979) is divergent. The Fredholm integral equation of the second kind in the paper of Eringen (Eringen, 1979) can be rewritten as following

$$h(x) + \int_0^1 h(u)L(x,u)\,du = g(x),$$

where $g(x)$ is known function, $h(x)$ is unknown function.

The kernel of the above Fredholm integral equation of the second kind can be written as follows:

$$L(x,u) = (xu)^{\frac{1}{2}} \int_0^\infty tk(\varepsilon t)J_0(xt)J_0(ut)\,dt, \quad 0 \leqslant x,u \leqslant 1,$$

where $J_n(x)$ is the Bessel function of order n.

$$k(\varepsilon t) = -\Phi(\varepsilon t), \quad \lim_{t\to\infty} k(\varepsilon t) \neq 0 \quad \text{for } \varepsilon = \frac{a}{2\beta l} \neq 0,$$

where l is the length of the crack,

$$J_0(x) \approx \sqrt{\frac{2}{\pi x}} \cos\left(x - \frac{1}{4}\pi\right) \quad \text{for } x \gg 0.$$

The limit of $tk(\varepsilon t)J_0(xt)J_0(ut)$ is not equal to zero for $t \to \infty$. So the kernel $L(x,u)$ in Eringen's paper is divergent (see e.g. Eringen, 1979). Of course, the dual integral equations can be considered to be a single integral equation of the first kind with a discontinuous kernel (see e.g. Eringen et al., 1977). It is well-known in the literature that integral equations of the first kind are generally ill-posed in sense of Hadamard, i.e. small perturbations of the data can yield arbitrarily large changes in the solution. This makes the numerical solution of such equations quite difficult. In this paper, Schmidt method (Morse and Feshbach, 1958) was used to overcome the difficulty. As discussed by Eringen's (Eringen et al., 1977; Eringen, 1977, 1978, 1979, 1983) and Nowinski's (Nowinski 1984a,b) papers, it was taken

$$\alpha_0 = \chi_0 \exp(-(\beta/a)^2(x' - x)^2), \quad \chi_0 = \beta/a\sqrt{\pi}, \tag{46}$$

where β is a constant (here β is a constant appropriate to each material) and a is the lattice parameter. So we obtain

$$\bar{\alpha}_0(s) = \exp(-(sa)^2/(2\beta)^2), \tag{47}$$

and $\bar{\alpha}_0(s) = 1$ for the limit $a \to 0$, so that Eqs. (41)–(44) reduce to the well-known equation of the classical theory. Here the Schmidt method can be used to solve the dual integral equations (41)–(44). The gap functions of the crack surface displacement are represented by the following series:

$$f_1(x) = w^{(1)}(x,0^+,t) - w^{(2)}(x,0^-,t) = \sum_{n=1}^\infty a_n P_{2n-2}^{(\frac{1}{2},\frac{1}{2})}\left(\frac{x}{l}\right)\left(1 - \frac{x^2}{l^2}\right)^{\frac{1}{2}}, \quad \text{for } -l \leqslant x \leqslant l, \quad y = 0, \tag{48}$$

$$f_1(x) = w^{(1)}(x,0^+,t) - w^{(2)}(x,0^-,t) = 0, \quad \text{for } |x| > l, \quad y = 0, \tag{49}$$

where a_n is unknown coefficients to be determined and $P_n^{(1/2,1/2)}(x)$ is a Jacobi polynomial (Gradshteyn and Ryzhik, 1980). The Fourier transform of Eq. (48) is (Erdelyi, 1954)

$$\bar{f}_1(s) = \sum_{n=1}^{\infty} a_n G_n \frac{1}{s} J_{2n-1}(sl), \quad G_n = 2\sqrt{\pi}(-1)^{n-1} \frac{\Gamma\left(2n - \frac{1}{2}\right)}{(2n-2)!}, \tag{50}$$

where $\Gamma(x)$ and $J_n(x)$ are the Gamma and Bessel functions, respectively.

Substituting Eq. (50) into Eqs. (41)–(44), respectively, the Eqs. (43) and (44) can be automatically satisfied. Then Eqs. (41) and (42) reduce to the form,

$$\sum_{n=1}^{\infty} a_n G_n \int_0^{\infty} \bar{\alpha}_0(s) \left\{ \mu \frac{\gamma}{s} [1 + e^{-\gamma h}] - \frac{e_{15}^2}{\varepsilon_{11}} [1 + e^{-sh}] \right\} J_{2n-1}(sl) \cos(sx) \, ds = \pi \tau_0. \tag{51}$$

For a large s, the integrands of the Eq. (51) are almost decreases exponentially. Hence they can be evaluated numerically by Filon's method (see e.g. Amemiya and Taguchi, 1969). Eq. (51) can now be solved for the coefficients a_n by the Schmidt method (Morse and Feshbach, 1958). For brevity, the Eq. (51) can be rewritten as

$$\sum_{n=1}^{\infty} a_n E_n(x) = U(x), \quad -l < x < l, \tag{52}$$

where $E_n(x)$ and $U(x)$ are known functions and the coefficients a_n are to be determined. A set of functions $P_n(x)$ which satisfy the orthogonality condition

$$\int_{-l}^{l} P_m(x) P_n(x) \, dx = N_n \delta_{mn}, \quad N_n = \int_{-l}^{l} P_n^2(x) \, dx \tag{53}$$

can be constructed from the function, $E_n(x)$, such that

$$P_n(x) = \sum_{i=1}^{n} \frac{M_{in}}{M_{nn}} E_i(x), \tag{54}$$

where M_{ij} is the cofactor of the element d_{ij} of D_n, which is defined as

$$D_n = \begin{bmatrix} d_{11}, d_{12}, d_{13}, \ldots, d_{1n} \\ d_{21}, d_{22}, d_{23}, \ldots, d_{2n} \\ d_{31}, d_{32}, d_{33}, \ldots, d_{3n} \\ \cdots\cdots\cdots\cdots \\ \cdots\cdots\cdots\cdots \\ \cdots\cdots\cdots\cdots \\ d_{n1}, d_{n2}, d_{n3}, \ldots, d_{nn} \end{bmatrix}, \quad d_{ij} = \int_{-l}^{l} E_i(x) E_j(x) \, dx. \tag{55}$$

Using Eqs. (52)–(55), we obtain

$$a_n = \sum_{j=n}^{\infty} q_j \frac{M_{nj}}{M_{jj}} \quad \text{with } q_j = \frac{1}{N_j} \int_{-l}^{l} U(x) P_j(x) \, dx. \tag{56}$$

5. Numerical calculations and discussion

From the works (see e.g. Itou, 1978, 1979; Zhou et al., 1999b; Zhou et al., 1998b; Zhou et al., 1999c; Zhou and Shen, 1999; Zhou and Jia, 2000), it can be seen that the Schmidt method is performed satisfactorily if the first ten terms of the infinite series of Eq. (52) are retained. The behavior of the stress stays steady with the increasing number of terms in (52). The coefficients a_n are known, so that the entire stress field and the electric displacement can be obtained. However, in fracture mechanics, it is important to determine the dynamic perturbation stress τ_{yz} and the perturbation electric displacement D_y in the vicinity of the crack's tips. τ_{yz} and D_y along the crack line can be expressed respectively as

$$\tau_{yz} = \tau_{yz}^{(1)}(x,0,t) = -\frac{1}{\pi}\sum_{n=1}^{\infty} a_n G_n \int_0^{\infty} \bar{\alpha}_0(s)\left\{\mu\frac{\gamma}{s}[1+\mathrm{e}^{-\gamma h}] - \frac{e_{15}^2}{\varepsilon_{11}}[1+\mathrm{e}^{-sh}]\right\} J_{2n-1}(sl)\cos(xs)\,\mathrm{d}s, \tag{57}$$

$$D_y = D_y^{(1)}(x,0,t) = -\frac{e_{15}}{\pi}\sum_{n=1}^{\infty} a_n G_n \int_0^{\infty} \bar{\alpha}_0(s)[1+\mathrm{e}^{-sh}] J_{2n-1}(sl)\cos(xs)\,\mathrm{d}s. \tag{58}$$

So long as the lattice parameter $a \neq 0$, the semi-infinite integration and the series in Eqs. (57) and (58) are convergent for any variable x. Eqs. (57) and (58) give finite stress and electric displacement all along $y = 0$, so there are no stress and the electric displacement singularity at the crack tips. However, for the lattice parameter $a = 0$, $\bar{\alpha}_0(s) = 1$, we have the classical stress singularity at the crack tips. At $-l < x < l$, $\tau_{yz}^{(1)}/\tau_0$ is very close to unity, and for $x > l$, $\tau_{yz}^{(1)}/\tau_0$ possesses finite values diminishing from a finite value at $x = l$ to zero at $x = \infty$. Since $a/2\beta l > 1/100$ represents a crack length of less than 100 atomic distances (as stated by Eringen, 1979), and such submicroscopic sizes other serious questions arise regarding the interatomic arrangements and force laws, we do not pursue solutions valid at such small crack sizes. The semi-infinite numerical integrals, which occur, are evaluated easily by Filon's method (see e.g. Amemiya and Taguchi, 1969) and Simpson's methods because of the rapid diminution of the integrands. In all computation, the piezoelectric materials are assumed to be the commercially available piezoelectric PZT-5H. The piezoelectric material constants of PZT-5H are $c_{44} = 2.3(\times 10^{10}$ N/m$^2)$, $e_{15} = 17.0$ (c/m^2) and $\varepsilon_{11} = 150.4(\times 10^{-10}$ C/Vm). The results of the dynamic stress field and the dynamic electric displacement field are plotted in Figs. 2–14. The results as shown in Figs. 2–14 are all of the problem that the electric boundary conditions are permeable. In Figs. 8 and 10, σ_{yz} and D_y^c represent the local stress and the local electric displacement, respectively. The following observations are very significant:

(i) The stress at the crack tip becomes infinite as the lattice parameter $a \to 0$. It is the classical continuum limit of square root singularity. This can be shown from Eqs. (41)–(44). For the lattice parameter $a \to 0$, $\bar{\alpha}_0(s) = 1$, Eqs. (41)–(44) will reduce to the dual integral equations for the same problem in classical piezoelectric materials. However, the stress and the electric displacement singularity are present at the crack tip in the local piezoelectric materials problem as well known.

(ii) For the $a/\beta =$ constant, viz., the atomic distance does not change, the value of the stress concentrations at the crack tip increase with increasing of the crack length ($a/2\beta l$ will decrease with increasing of the crack length l). Experiments indicate that the piezoelectric materials with smaller cracks are more resistant to fracture than those with larger cracks.

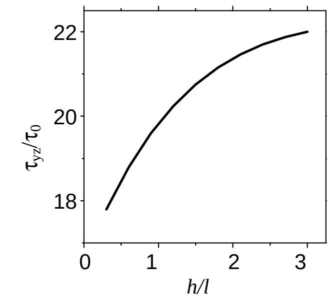

Fig. 2. The stress at the crack tip versus h/l for $l = 1.0$, $a/2\beta l = 0.0005$, $\omega l/c = 0.2$.

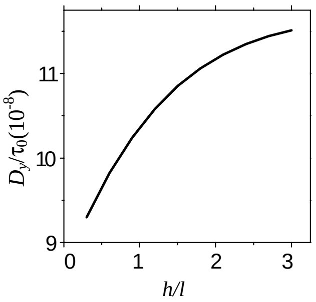

Fig. 3. The electric displacement at the crack tip versus h/l for $\omega l/c = 0.2$, $a/2\beta l = 0.0005$, $l = 1.0$.

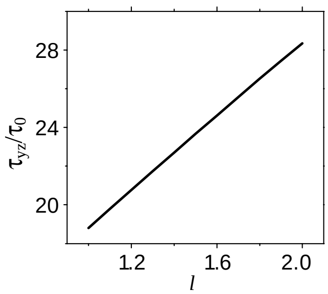

Fig. 4. The stress at the crack tip versus l for $\omega l/c = 0.2$, $a/2\beta l = 0.0005$, $h/l = 0.6$.

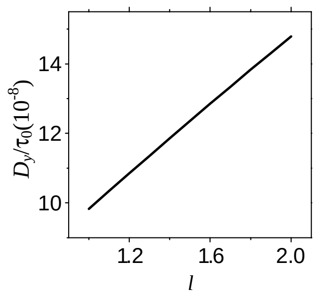

Fig. 5. The electric displacement at the crack tip versus l for $\omega l/c = 0.2$, $a/2\beta l = 0.0005$, $h/l = 0.6$.

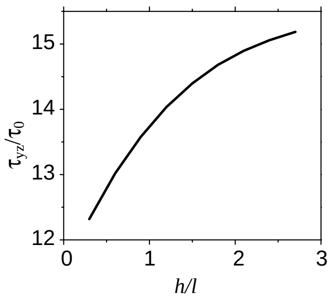

Fig. 6. The stress at the crack tip versus h/l for $l = 1.0$, $a/2\beta l = 0.001$, $\omega l/c = 0.2$.

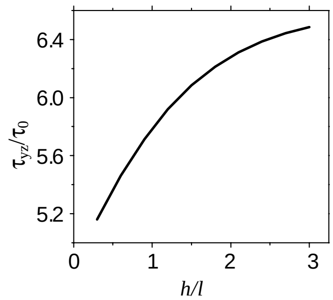

Fig. 7. The stress at the crack tip versus h/l for $l = 1.0$, $a/2\beta l = 0.005$, $\omega l/c = 0.6$.

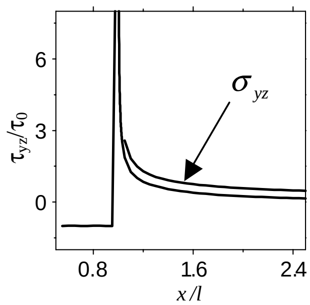

Fig. 8. The stress along the crack line versus x/l for $\omega l/c = 0.2$, $l = 1.0$, $a/2\beta l = 0.0005$, $h/l = 0.6$.

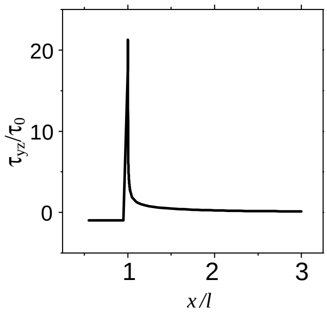

Fig. 9. The stress along the crack line versus x/l for $\omega l/c = 0.2$, $l = 1.0$, $a/2\beta l = 0.0005$, $h/l = 0.6$.

(iii) The significance of this result is that the fracture criteria are unified at both the macroscopic and microscopic scales, viz., it may solve the problem of any scale cracks (it may solve the problem of any value of $a/2\beta l$).
(iv) The present results will revert to the classical ones for $\alpha(|X' - X|) = \delta(|X' - X|)$.
(v) The results of the stress and the electric displacement at the crack tip tend to decrease with increasing of the lattice parameter a.
(vi) The stress and the electric displacement at the crack tip increase with increasing of the distance between two parallel cracks as shown in Figs. 2, 3, 6 and 7. This phenomenon is called crack shielding effect.

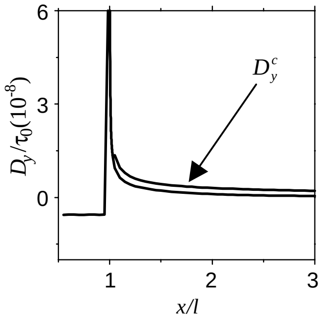

Fig. 10. The electric displacement along the crack line versus x/l for $\omega l/c = 0.2$, $a/2\beta l = 0.0005$, $h/l = 0.6$, $l = 1.0$.

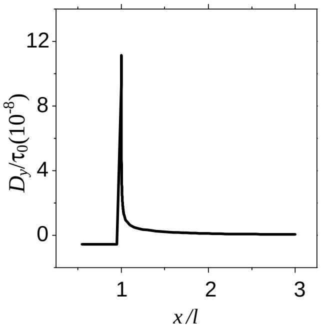

Fig. 11. The electric displacement along the crack line versus x/l for $\omega l/c = 0.2$, $a/2\beta l = 0.0005$, $h/l = 0.6$, $l = 1.0$.

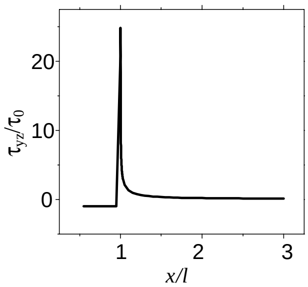

Fig. 12. The stress along the crack line versus x/l for $\omega l/c = 0.2$, $l = 1.0$, $a/2\beta l = 0.0005$, $h/l = 1.5$.

(vii) The stress and the electric displacement at the crack tip increase almost linearity with increase of the crack length as shown in Figs. 4 and 5.

(viii) For the lattice parameter $a \neq 0$, it can be proved that the semi-infinite integration in Eqs. (57) and (58) and the series in Eqs. (57) and (58) are convergent for any variable x. Therefore the dynamic stress and the dynamic electric displacement give finite values all along the crack line. Contrary to the classical piezoelectric theory solution, it is found that no stress and electric displacement singularity are present at the crack tip, and the present results converge to the classical ones far away from the crack tip as shown in Figs. 8 and 10. The maximum stress does not occur at the crack tip, but slightly

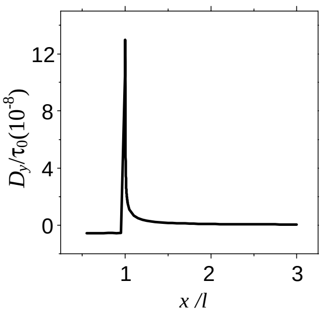

Fig. 13. The electric displacement along the crack line versus x/l for $\omega l/c = 0.2$, $a/2\beta l = 0.0005$, $h/l = 1.5$, $l = 1.0$.

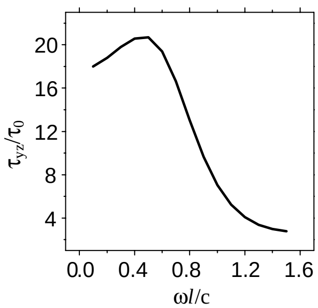

Fig. 14. The stress at the crack tip versus $\omega l/c$ for $l = 1.0$, $a/2\beta l = 0.0005$, $h/l = 0.6$.

away from it. This phenomenon has been thoroughly substantiated by Eringen (Eringen, 1983). The distance between the crack tip and the maximum stress point is very small, and it depends on the crack length and the lattice parameter.

(ix) From the results of Zhou's paper (Zhou et al., 2001) and the present paper, it can be found that the electric displacement of the permeable crack surface conditions problem is much smaller than the result of the impermeable crack surface conditions problem.

(x) The dynamic stress and the electric displacement at the crack tips tend to increase with frequency reaches a peak, then decreases in magnitude. So the dynamic field will impede or enhance crack propagation in a piezoelectric material depending on the circular frequency of the incident wave as shown in Fig. 14.

Acknowledgements

The authors are grateful for financial supported by the Natural Science Foundation of Hei Long Jiang Province, the National Natural Science Foundation of China Through the Key Program (50232030), the National Natural Science Foundation of China (10172030), the Post Doctoral Science Foundation of Hei Long Jiang Province and the Multidisciline Scientific Research Foundation of Harbin Institute of Technology (HIT.MD.2002.39).

References

Amemiya, A., Taguchi, T., 1969. Numerical analysis and fortran. Maruzen, Tokyo.

Beom, H.G., Atluri, S.N., 1996. Near-tip fields and intensity factors for interfacial cracks in dissimilar anisotropic piezoelectric media. International Journal of Fracture 75, 163–183.

Chen, Z.T., Karihaloo, B.L., Yu, S.W., 1999. Dynamic response of a cracked piezoelectric ceramic under arbitrary electro-mechanical impact. International Journal of Solids and Structures 36, 5125–5133.

Deeg, W.E.F., 1980. The analysis of dislocation, crack and inclusion problems in piezoelectric solids, Ph.D. thesis, Stanford University.

Dunn, M.L., 1994. The effects of crack face boundary conditions on the fracture mechanics of piezoelectric solids. Engineering Fracture of Mechanics 48, 25–39.

Erdelyi, A. (Ed.), 1954. Tables of integral transforms, vol. 1. McGraw-Hill, New York, p. 38, 94.

Eringen, A.C., 1974. Non-local elasticity and waves. In: Thoft-Christensen, P. (Ed.), Continuum Mechanics Aspects of Geodynamics and Rock Fracture Mechanics. Dordrecht, Holland, pp. 81–105.

Eringen, A.C., 1977. Continuum mechanics at the atomic scale. Crystal Lattice Defects 7, 109–130.

Eringen, A.C., 1978. Linear crack subject to shear. International Journal of Fracture 14, 367–379.

Eringen, A.C., 1979. Linear crack subject to antiplane shear. Engineering Fracture Mechanics 12, 211–219.

Eringen, A.C., 1983. Interaction of a dislocation with a crack. Journal of Applied Physics 54, 6811.

Eringen, A.C., 1984. Theory of non-local piezoelectricity. Journal of Mathematics and Physics 23 (3), 717–727.

Eringen, A.C., Speziale, C.G., Kim, B.S., 1977. Crack tip problem in non-local elasticity. Journal of Mechanics and Physics of Solids 25, 339–355.

Gao, H., Zhang, T.Y., Tong, P., 1997. Local and global energy rates for an elastically yielded crack in piezoelectric ceramics. Journal of Mechanics and Physics of Solids 45, 491–510.

Gradshteyn, I.S., Ryzhik, I.M., 1980. Table of integral, series and products. Academic Press, New York, p. 1035.

Han, X.-L., Wang, T., 1999. Interacting multiple cracks in piezoelectric materials. International Journal of Solids and Structures 36, 4183–4202.

Itou, S., 1978. Three dimensional waves propagation in a cracked elastic solid. ASME Journal of Applied Mechanics 45, 807–811.

Itou, S., 1979. Three dimensional problem of a running crack. International Journal of Engineering Science 17, 59–71.

Kim, S.J., Jones, J.D., 1996. Effects of piezo-actuator delamination on the performance of active noise and vibration control system. Journal of Intelligent Material Systems and Structures 7, 668–676.

McMeeking, R.M., 1989. On mechanical stress at cracks in dielectrics with application to dielectric breakdown. Journal of Applied Physics 62, 3316–3322.

Morse, P.M., Feshbach, H., 1958. Methods of theoretical physics, vol. 1. McGraw-Hill, New York.

Narita, K., Shindo, Y., 1998. Anti-plane shear crack growth rate of piezoelectric ceramic body with finite width. Theoretical and Applied Fracture Mechanics 30, 127–132.

Nowinski, J.L., 1984a. On non-local aspects of the propagation of love waves. International Journal of Engineering Science 22, 383–392.

Nowinski, J.L., 1984b. On non-local theory of wave propagation in elastic plates. ASME Journal of Applied Mechanics 51, 608–613.

Pak, Y.E., 1990. Crack extension force in a piezoelectric material. Journal of Applied Mechanics 57, 647–653.

Pak, Y.E., 1992. Linear electro-elastic fracture mechanics of piezoelectric materials. International Journal of Fracture 54, 79–100.

Park, S.B., Sun, C.T., 1995. Effect of electric field on fracture of piezoelectric ceramics. International Journal of Fracture 70, 203–216.

Qin, Q.H., Yu, S.W., 1997. An arbitrarily-oriented plane crack terminating at the interaction between dissimilar piezoelectric materials. International Journal of Solids and Structures 34, 581–590.

Shen, S., Kuang, Z.B., Hu, S., 1999. On interface crack in laminated anisotropic medium. International Journal of Solids and Structures 36, 4251–4268.

Shen, S., Nishioka, T., Kuang, Z.B., Liu, Z.X., 2000. Non-linear electromechanical interfacial fracture for piezoelectric materials. Mechanics of Materials 32, 57–64.

Shindo, Y., Narita, K., Tanaka, K., 1996. Electroelastic intensification near anti-plane shear crack in orthotropic piezoelectric ceramic strip. Theoretical and Applied Fracture Mechanics 25, 65–71.

Soh, A.K., Fang, D.N., Lee, K.L., 2000. Analysis of a bi-piezoelectric ceramic layer with an interfacial crack subjected to anti-plane shear and in-plane electric loading. European Journal of Mechanics. A/Solid 19, 961–977.

Sosa, H., 1991. Plane problems in piezoelectric media with defects. International Journal of Solids and Structures 28, 491–505.

Sosa, H., 1992. On the fracture mechanics of piezoelectric solids. International Journal of Solids and Structures 29, 2613–2622.

Sosa, H.A., Pak, Y.E., 1990. Three-dimensional eigenfunction analysis of a crack in a piezoelectric ceramics. International Journal of Solids and Structures 26, 1–15.

Sosa, H., Khutoryansky, N., 1999. Transient dynamic response of piezoelectric bodies subjected to internal electric impulses. International Journal of Solids and Structures 36, 5467–5484.

Srivastava, K.N., Palaiya, R.M., Karaulia, D.S., 1983. Interaction of shear waves with two coplanar Griffith cracks situated in an infinitely long elastic strip. International Journal of Fracture 23, 3–14.

Suo, Z., 1993. Models for breakdown-resistant dielectric and ferroelectric ceramics. Journal of the Mechanics and Physics of Solids 41, 1155–1176.

Suo, Z., Kuo, C.-M., Barnett, D.M., Willis, J.R., 1992. Fracture mechanics for piezoelectric ceramics. Journal of Mechanics and Physics of Solids 40, 739–765.

Wang, B., 1992. Three dimensional analysis of a flat elliptical crack in a piezoelectric material. International Journal of Engineering Science 30 (6), 781–791.

Yu, S.W., Chen, Z.T., 1998. Transient response of a cracked infinite piezoelectric strip under anti-plane impact. Fatigue and Engineering Materials and Structures 21, 1381–1388.

Zhang, T.Y., Hack, J.E., 1992. Mode-III cracks in piezoelectric materials. Journal of Applied Physics 71, 5865–5870.

Zhang, T.Y., Tong, P., 1996. Fracture mechanics for a mode III crack in a piezoelectric material. International Journal of Solids and Structures 33, 343–359.

Zhou, Z.G., Jia, D.B., 2000. The scattering of harmonic elastic anti-plane waves by two collinear symmetric cracks in infinite long strip using the non-local theory. Mechanics Research Communication. 27 (3), 307–318.

Zhou, Z.G., Shen, Y.P., 1999. Investigation of the scattering of harmonic shear waves by two collinear cracks using the non-local theory. ACTA Mechanica 135, 169–179.

Zhou, Z.G., Han, J.C., Du, S.Y., 1998a. Non-local theory solution for in-plane shear of through crack. Theoretical and Applied Fracture Mechanics 30, 185–194.

Zhou, Z.G., Wang, B., Du, S.Y., 1998b. Investigation of the scattering of harmonic elastic anti-plane shear waves by a finite crack using the non-local theory. International Journal of Fracture 91, 13–22.

Zhou, Z.G., Bai, Y.Y., Zhang, X.W., 1999a. Scattering of harmonic shear waves by a finite crack by using the non-local theory. International Journal of Engineering Science 37 (5), 609–620.

Zhou, Z.G., Han, J.C., Du, S.Y., 1999b. Investigation of a Griffith crack subject to anti-plane shear by using the non-local theory. International Journal of Solids and Structures 36, 3891–3901.

Zhou, Z.G., Bai, Y.Y., Zhang, X.W., 1999c. Two collinear Griffith cracks subjected to uniform tension in infinitely long strip. International Journal of Solids and Structures 36, 5597–5609.

Zhou, Z.G., Du, S.Y., Wang, B., 2001. Investigation of anti-plane shear behavior of a Griffith crack in a piezoelectric materials by using the non-local theory. International Journal of Fracture 111, 105–117.